

Assessment of texture features for Brazilian savanna classification: a case study in Brasilia National Park

Cesare Di Girolamo Neto¹, Leila Maria Garcia Fonseca¹, Thales Sehn Körting¹

¹Instituto Nacional de Pesquisas Espaciais – INPE
Caixa Postal 515 - 12227-010, São José dos Campos – SP – Brazil

{cesare.neto;leila.fonseca; thales.korting}@inpe.br

Abstract. *Distinguishing Brazilian savanna physiognomies is an essential task to better evaluate carbon storage and potential emissions of greenhouse gases. In this study, we propose to evaluate the potential of texture features to improve the discrimination among five physiognomies in the Brazilian savanna: Open Grasslands, Shrubby Grassland, Shrubby Savanna, Savanna Woodland and Gallery Forest. Texture features extracted from RapidEye images and also from Spectral Linear Mixture Model components and Vegetation Index are evaluated in this study. Results showed that texture features based on GLCM can reduce misclassification for Open Grasslands, Shrubby Grasslands and Shrubby Savanna classes.*

1. Introduction

Brazilian savanna, also known as Cerrado, occupies an area of approximately two million square Kilometers on the Brazilian territory, mainly in the central part of Brazil (MMA, 2015). Cerrado is one of the richest biomes in the world and it contains more than 160.000 species of plants, animals and fungi (Ferreira *et al.*, 2003). Besides that, Cerrado is responsible for storing about 5.9 billion tons of carbon in vegetation and 23.8 billion tons in the ground (MMA, 2014).

The loss of natural vegetation in Cerrado reached 45.5% of its original area by 2013 (MMA, 2015). The loss of biodiversity can lead to problems such as: soil erosion, water pollution, carbon cycle of instability, microclimate changes and also biome fragmentation (Klink & Machado, 2005). Considering these negative effects on biodiversity, it is essential to promote strategies to monitor the Cerrado biome.

Mapping of heterogeneous tropical areas, such as Cerrado, should be carried out considering biological, climatic and topographical information. The major natural formations in Cerrado are Grasslands, Shrublands and Woodlands (Figure 1). Their mapping has been the subject of several studies. Sano *et al.* (2009) performed visual interpretation of satellite images to produce maps of Cerrado. This process was very time consuming and difficult to discriminate Grasslands.

The difficulty to map Cerrado patterns is even greater when considering more formations than those mentioned above. For example, the system proposed by Ribeiro & Walter (2008) splits these major formations into 14 physiognomies. Identifying these physiognomies is important to evaluate carbon storage and potential emissions of greenhouse gases for each type of land cover.

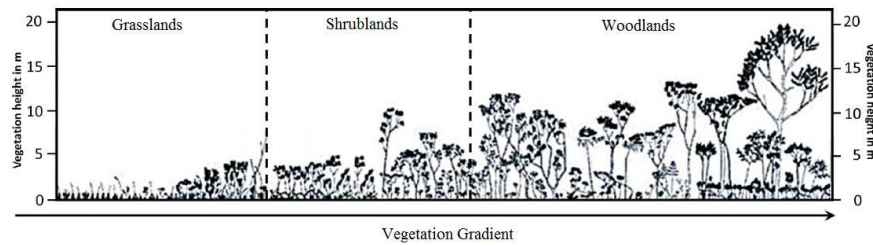


Figure 1. Major Cerrado formations describing the vegetation gradient (adapted from Schwieder *et al.*, 2016).

Most studies aiming to classify vegetation types in the Cerrado biome rely on the use of spectral information from remote sensing imagery. The NDVI (Normalized Difference Vegetation Index) has been tested to discriminate Cerrado physiognomies (Liesenberg *et al.*, 2007; Oliveira *et al.*, 2007; Costa *et al.*, 2014). However, there is still difficulty to discriminate different grassland physiognomies using only NDVI. Spectral Linear Mixture Model (SLMM) has also been used to classify physiognomies on a protected area of Cerrado in Distrito Federal State, Brazil (Ferreira *et al.*, 2007). The SLMM reduced the classification error between Grasslands and Shrublands, but it was not enough to fully automate the classification.

Differently, Carvalho *et al.* (2010) used texture features to map the vegetation cover in the Cerrado. In this paper, an initial classification was performed using data based on NDVI, SLMM and spectral features. Afterwards, they included texture information into the dataset and noticed an increase in the classification accuracy. Peneque-Galvez *et al.* (2013) also used texture features to classify Cerrado physiognomies in Bolivia. In this case, Woodlands were classified with high accuracy, but some errors confusion occurred in the discrimination between Grasslands and Shrublands. However, some texture features increased this error, and reduced the overall classification accuracy. Therefore, it is necessary to investigate whether these features may be really effective for Cerrado classification.

In order to better analyze texture features in the Cerrado classification, we could calculate texture features from NDVI instead of calculating it from original image. The NDVI texture has been used in other applications such as urban studies (Nussbaum & Menz, 2008). It has also been used to detect bushfire prone areas (Chen *et al.*, 2001) as well as to identify different types of forest and spatial patterns of vegetation structure (Ning *et al.*, 2011).

Therefore, we propose in this work to evaluate the potential use of texture information extracted from RapidEye original images, and also from vegetation index and SLMM components to classify the following physiognomies in the Brazilian Cerrado: Open Grasslands, Shrubby Grassland, Shrubby Savanna, Savanna Woodland and Gallery Forest.

2. Methodology

Figure 2 presents the methodology flowchart proposed to classify vegetation cover in Cerrado. Each processing step is detailed in the following sections.

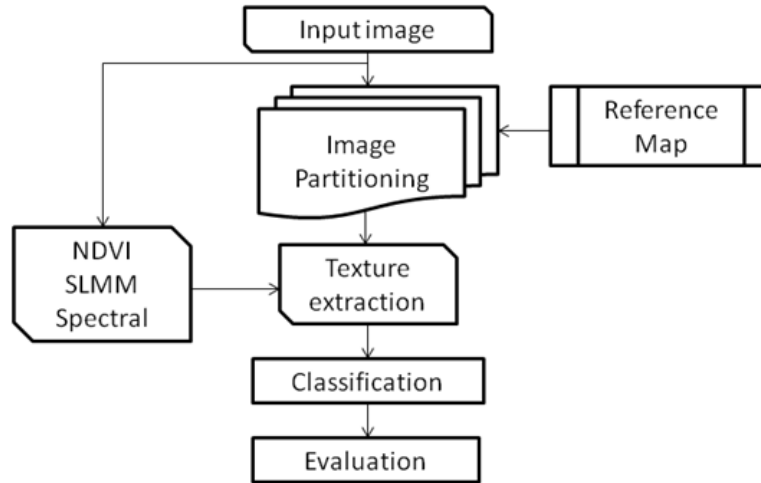


Figure 2: Methodology flowchart.

2.1. Study Area and Reference Map

The study area is located in the Brasília National Park (PNB), which has approximately 30.000 ha of preserved natural Cerrado vegetation. Figure 3 shows the major part of the park, in which a red line highlights the study area. For the experiments, we used a RapidEye image in the path-row 1-318 tile 2331801 of the RapidEye Earth Imaging System (REIS). This image was acquired in 05/30/2014 and processed in level 3A product (Blackbridge, 2015).

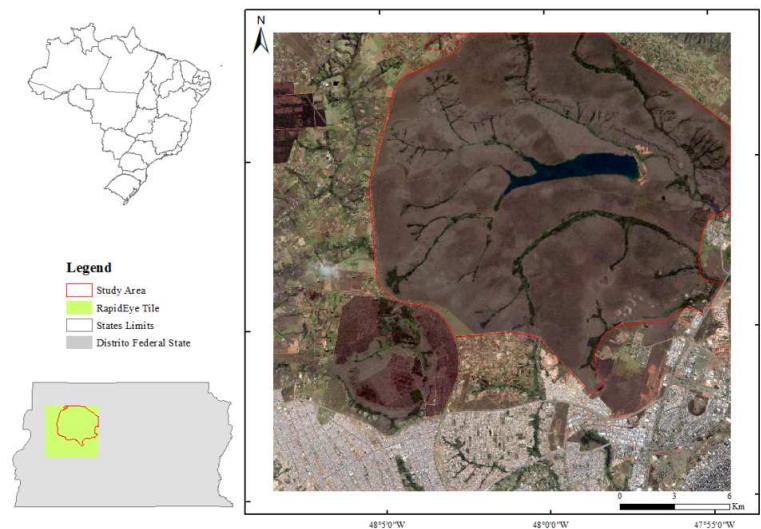


Figure 3: Study area in the Brasilia National Park.

We also used as reference the map of PNB that was produced by Ferreira *et al.* (2007). The authors used the system proposed by Ribeiro & Walter (1998) to classify 5 Cerrado physiognomies described in Table 1. Other classes such as Water Bodies, Marsh, Reforestation, Bare Soil and Constructed Area were removed from the dataset.

Table 1. Cerrado physiognomies characteristics (Adapted from Ferreira *et al.*, 2007 and Ribeiro & Walter, 2008)

<i>Physiognomy name</i>	<i>Vegetation description</i>	<i>Tree cover (%)</i>	<i>Tree height (m)</i>
Open Grassland (OG)	Grasses	0	-
Shrubby Grassland (SG)	Grasses and Shrubs	0-5	-
Shrubby Savanna (SS)	Shrubs and a few trees	5-20	2-3
Wooded Savanna (WS)	Trees and a few Shrubs	20-50	3-6
Gallery Forest (GF)	Trees	70-95	15-30

2.2. Image Partitioning

In order to extract texture features, the image was partitioned into square objects of size s by s pixels. The use of square objects instead of polygons extracted from segmentation algorithms based on similarity allows us to evaluate texture features that capture the natural heterogeneity in the image. This procedure prevents detecting texture as a possible rule in the classification process, once we intend to evaluate texture potential for classifying Cerrado vegetation cover.

Following, the image was linked with the reference map to identify the square objects represented within each class in the map. The larger is the square object size, the fewer number of objects can be extracted from the image. We tested different object sizes ranging from 10 to 35, with a step of 5. The maximum value 35 was chosen because the number of samples for Gallery Forest reached almost zero. Figure 4 illustrates the influence of object size in relation to the number of samples for Gallery Forest.

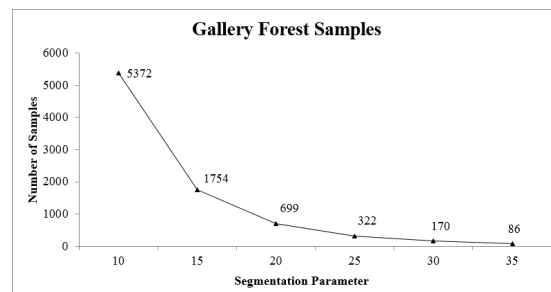


Figure 4. The influence of objects size in relation to the number of samples of Gallery Forest.

After partitioning process, some segments presented two or more classes, which can lead to misclassification (Ferreira *et al.*, 2007, Oliveira *et al.*, 2007 and Carvalho *et al.*, 2010). To reduce this problem these elements were removed from the dataset. Figure 6 illustrates this procedure of cleaning up.

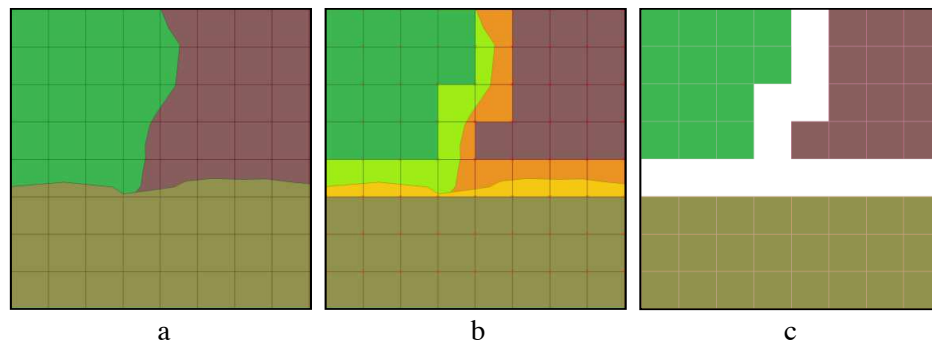


Figure 6. Clean up process. a) original map with 3 different classes; b) highlighted objects for removal; c) map of samples after cleanup process.

2.3. Feature Extraction

Spectral features were obtained from Digital Numbers (DN) of RapidEye (RE) bands. The description the spectral features is presented in Table 2.

Table 2. Spectral Features.

Feature	Description
Band_1	DN from band 1 (Blue 440 – 510 μm)
Band_2	DN from band 2 (Green 520 – 590 μm)
Band_3	DN from band 3 (Red 630 – 685 μm)
Band_4	DN from band 4 (Red Edge 690 – 730 μm)
Band_5	DN from band 5 (NIR 760 – 810 μm)
Brightness (BT)	Average of the sum of means for bands 1-5
Maximum Difference (MD)	Maximum of the difference between bands
NDVI	Normalized Difference Vegetation Index
SLMM_soil	SLMM component of soil
SLMM_shadow	SLMM component of shadow
SLMM_vegetation	SLMM component of vegetation

NDVI and SLMM components (*soil*, *shadow* and *vegetation*) were computed according to Tucker (1979) and Shimabukuro & Smith (1991), respectively. Texture features were computed from Gray Level Co-occurrence Matrix (GLCM) as shown in Table 3. GLCM is a second order histogram in which each entry reports the joint probability of finding a set of two grey levels at a certain distance and direction from each other over some pre-defined window (Haralick *et al.*, 1973). Additionally, some texture measures were computed from Gray Level Difference Vector (GLDV), as shown in Table 3. GLDV indicates occurrence of the absolute difference between a reference pixel and its neighbor. It can be calculated for 4 different directions (0°, 45°, 90° and 135°). In this study, we used only direction 0°.

Texture features were also extracted from image bands, from NDVI, and from each SLMM component (*soil*, *shadow* and *vegetation*). Therefore, 9 texture features (Table 3) were extracted from five images (vector of bands, NDVI, SLMM), which produced a total of 45 features. The features of BT and MD were not used for extracting texture.

Table 3. Textural features based on (Haralick *et al.*, 1973). $P_{i,j}$ is the normalized co-occurrence matrix, N is the number of rows or columns, σ_i and σ_j are standard deviation of row i and column j , μ_i and μ_j are means of row i and column j , V_k is the normalized gray level difference vector, and $k = |i-j|$.

Feature	Formula	Feature	Formula
GLCM Entropy	$\sum_{i,j=0}^{N-1} P_{i,j} (-\ln P_{i,j})$	GLCM Dissimilarity	$\sum_{i,j=0}^{N-1} P_{i,j} i-j $
GLDV Entropy	$\sum_{k=0}^{N-1} V_k (-\ln V_k)$	GLCM Homogeneity	$\sum_{i,j=0}^{N-1} \frac{P_{i,j}}{1+(i-j)^2}$
GLCM Contrast	$\sum_{i,j=0}^{N-1} P_{i,j} (i-j)^2$	GLCM Mean	$\mu_i = \sum_{i,j=0}^{N-1} i (P_{i,j})$
GLDV Contrast	$\sum_{k=0}^{N-1} V_k (k^2)$	GLDV Mean	$\mu_i = \sum_{i,j=0}^{N-1} V_k (k)$
GLCM Correlation	$\sum_{i,j=0}^{N-1} P_{i,j} \left[\frac{(1-\mu_i)(1-\mu_j)}{\sqrt{(\sigma_i)^2 (\sigma_j)^2}} \right]$		

2.4. Classification

In the classification phase we performed two experiments. In the first experiment, we used four datasets in the classification phase, as shown in Table 4. This was the baseline to evaluate the classification accuracy gain by including each feature into the datasets one at a time. The idea of this experiment is to evaluate classification accuracy for each spectral feature and also the spectral texture, which has been pointed out by Carvalho *et al.* (2010) and Peneque-Galvez *et al.* (2013) as features that improve Cerrado classification. In Table 4, Spectral Texture means texture features extracted from RapidEye bands only.

Table 4: Combination of groups of features to evaluate the best subset for classification.

	RE bands, BT, MD	NDVI	SLMM	Spectral Texture
Dataset 1	X			
Dataset 2	X	X		
Dataset 3	X	X	X	
Dataset 4	X	X	X	X

In the experiment 2, we evaluated all 45 texture features, adding one at a time in each one of the datasets 1-3. The idea was to evaluate the improvement or not in the classification accuracy for each texture feature.

For comparison, we established the same classification algorithm and parameters for all tests. We used Random Forest classification algorithm (Breiman, 2001),

implemented in Weka software (Hall *et al.*, 2009), and set the number of trees to 100 in order to construct each forest.

2.5. Texture Feature Evaluation

The experiments were carried out using a 10-fold cross validation. For the validation process, we used Global Accuracy, Precision and Recall values to summarize the confusion matrix in the experiments:

$$Global\ Accuracy = \frac{TP + TN}{n} \quad (1)$$

$$Precision = \frac{TP}{(TP + FP)} \quad (2)$$

$$Recall = \frac{TP}{(TP + FN)} \quad (3)$$

in which TP = True Positive, FP = False Positive, TN = True Negative, FN = False Negative and n = number of samples. Recall and Precision mean, respectively, percentage of instances of one class that are correctly classified and the map accuracy.

We proposed a ranking system to evaluate the inclusion of textural features into the datasets. It is based on accuracy percentage gain (or loss), *Acc*, when a certain feature is added into the dataset:

$$Acc = \frac{Acc_f}{Acc_i} \quad (3)$$

in which *Acc* is the accuracy percentage gain, *Acc_i* is the initial accuracy and *Acc_f* is the accuracy when a texture feature is included in the set of features.

Each one of the 45 features were ranked from 1-45, being 1 the feature that presented more percentage gain and so on. This was performed for datasets 1-3 and segmentation of size equal to 30. A final rank considered the average performance. Table 5 shows an example of this ranking for 3 hypothetical features.

Table 5: Ranking system example for 3 hypothetical features.

Dataset #	1	2	3	Average rank	Final Rank
Feature 1 Rank	1st	1st	1st	1,00	1st
Feature 2 Rank	2nd	2nd	3rd	2,33	2nd
Feature 3 Rank	3rd	3rd	2nd	2,66	3rd

3. Results

This section presents results obtained from two experiments mentioned in section 2.4.

3.1. Experiment 1: spectral texture features analysis

Figure 7 presents the accuracy classification for all 4 datasets (Table 3) in relation to the segmentation parameter *s*. We observe that for datasets 1, 2 and 3, the classification values did not presented meaningful difference. That is, the addition of NDVI and SLMM features into the feature set did not improve the classification result. Nevertheless, inclusion of spectral texture features (dataset 4) improved the classification result, which corroborates with Carvalho *et al.* (2010) and

Peneque-Galvez *et al.* (2013). Another observation is that the classification for segmentation parameter equals to 30 presented better result than the others (Figure 7).

In order to better investigate this result, we evaluated Precision and Recall values for each class for the classification for the segmentation parameter of 30 (Table 7). We can observe that Shrubby Savanna (SS) and Shrubby Grassland (SG) classes presented the worst classification. Open Grassland (OG) and Wooded Savanna (WS) presented better precision values, but not as good as the ones for Gallery Forest (GF) class. GF class is the only physiognomy with forest structure and it was expected that it would present better classification accuracy than the others.

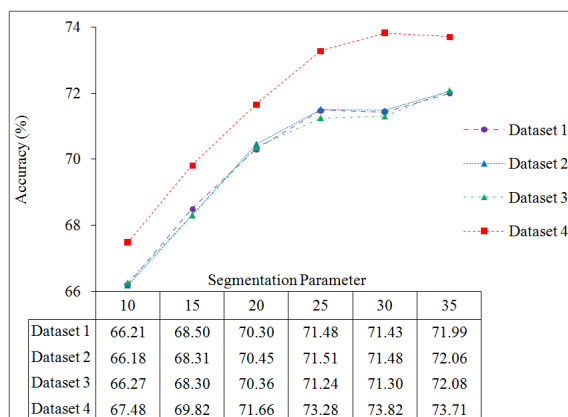


Figure 7: Accuracy values (%) for datasets 1-4 according to the segmentation parameter.

When spectral texture is added, we noticed an increase in the recall values for all classes, except for GF. The SG class presented the highest precision gains when spectral texture was added. Oliveira *et al.* (2007) pointed out that discrimination between OG and SG classes is difficult. Costa *et al.* (2014) even suggested merging both classes to decrease classification error. Ferreira *et al.* (2007) also reported confusion between SG and SS classes. However, our results show that the use of spectral texture can improve considerably their discrimination.

Table 7. Precision (P) and Recall (R) values for each class from dataset 1 and 4 for the segmentation parameter of 30.

	Open Grassland		Shrubby Grassland		Shrub Savanna		Wooded Savanna		Gallery Forest		Accuracy
	P	R	P	R	P	R	P	R	P	R	
Dataset1	0,761	0,829	0,519	0,411	0,620	0,510	0,761	0,827	0,947	0,941	71,43
Dataset4	0,757	0,866	0,578	0,486	0,666	0,507	0,781	0,842	0,970	0,935	73,82

3.2. Experiment 2: texture features analyses

In this part, we analyze the texture potential of improving the classification in relation to the 5 cerrado classes and $s = 30$. As mentioned on section Section 2.4, each of the 45 texture features were added separately on datasets 1-3. Final rank of the best features is presented in Table 8.

Table 8. Ranking the 10 best texture features. *Vegetation, shadow and soil* represent the features obtained from SLMM images.

Feature Name	Average Rank	Final Rank
GLCM Entropy <i>vegetation</i>	1,3	1st
GLCM Entropy NDVI	2,3	2nd
GLCM Entropy <i>shadow</i>	2,6	3rd
GLCM Entropy <i>soil</i>	4,6	4th
GLDV Entropy spectral	9,6	5th
GLCM Contrast <i>shadow</i>	10,0	6th
GLCM Contrast spectral	11,0	7th
GLDV Contrast <i>shadow</i>	11,0	
GLCM Dissimilarity spectral	11,0	
GLCM Corre <i>shadow</i>	11,6	10th

Considering SLMM components and NDVI, the best ranks were achieved by 'GLCM Entropy' features. Homogeneous objects have high entropy values while heterogeneous ones have low entropy. In Cerrado, tree density and canopy formation are responsible for making an object more or less homogeneous.

Figure 8 shows the mean values for the “GLCM Entropy *vegetation*” for the five Cerrado physiognomies. It shows us that, SG and SS classes presented the lowest mean values for 'GLCM Entropy *vegetation*'. Although SG does not have continuous canopy it presents bushes more frequently when compared to OG. This makes SG less homogeneous than OG and, therefore, producing lower entropy vegetation than OG. Regarding to SS class, Ribeiro and Walter (2008) stated that there is a canopy formation, however it is much sparser and with a lower tree cover percentage than the WS class. These vegetation patterns were captured by features such as “GLCM Entropy *vegetation*” and “GLCM Entropy NDVI”, which achieved the best rankings (1st and 2nd, respectively).

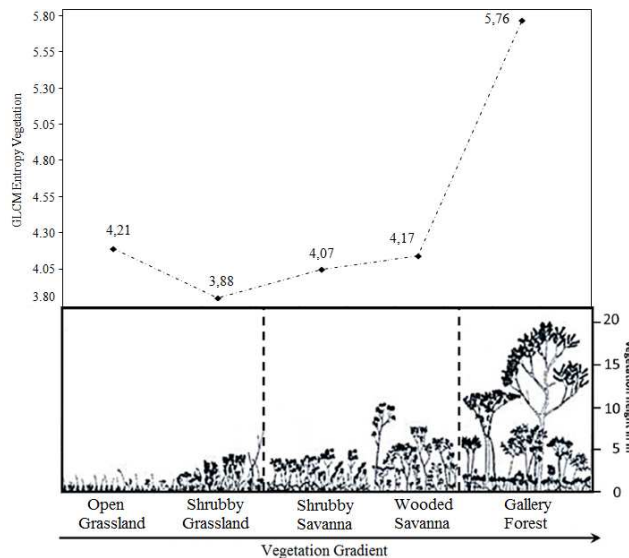


Figure 8: GLCM Entropy *vegetation* mean values for Cerrado physiognomies (adapted from Schwieder *et al.*, 2016).

Table 10 presents Recall and Precision values when “GLCM Entropy vegetation”, first feature in the ranking, was added to dataset 3. We noticed a slightly classification improvement for all classes, except for GF Precision. The SG and OG classes presented a little increase in the Recall values. The use of features such as ‘GLCM Entropy vegetation’ and ‘GLCM Entropy NDVI’ improved the discrimination of both classes, as can be noticed in Recall values. We also observed a little improvement of Recall values for SS class.

Table 10. Precision (P) and Recall (R) for each class with addition of textural entropy.

	Open Grassland		Shrubby Grassland		Shrub Savanna		Wooded Savanna		Gallery Forest	
	P	R	P	R	P	P	R	P	R	P
Dataset3	0,760	0,824	0,516	0,450	0,611	0,504	0,763	0,824	0,958	0,941
+ GLCM Entropy vegetation	0,782	0,864	0,567	0,488	0,649	0,529	0,791	0,846	0,936	0,953

Figure 9 shows an example of how important is to correctly choose the best features to improve the classification accuracy. GLCM Entropy features were much more consistent than the others in all classifications, obtaining always the best ranking. Using some texture features may not really improve the classification results as mentioned by Peneque-Galvez *et al.* (2013).

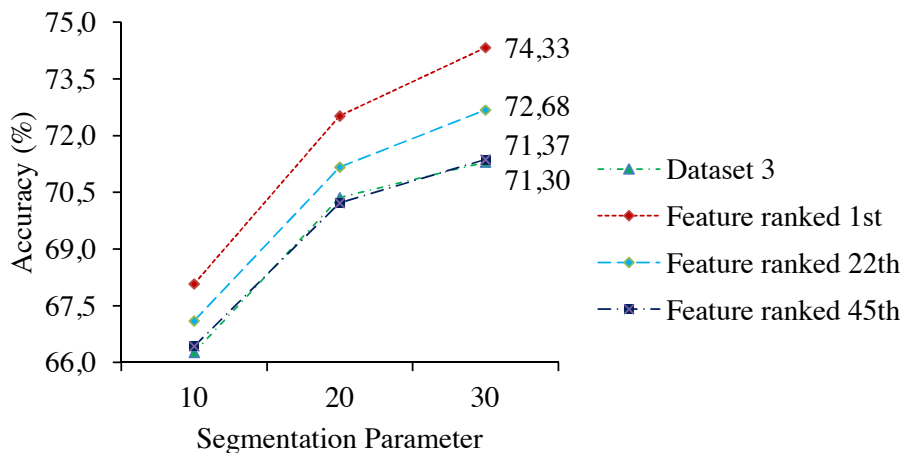


Figure 9. Influence of some features in the final classification accuracy. Feature ranked as 1st is “GLCM Entropy vegetation”, 22th is “GLDV Contrás NDVI” and 45th is “GLCM Mean spectral”.

4. Conclusion

In this study, we presented the assessment of texture features (spectral, NDVI and SLMM) to improve the discrimination of Cerrado physiognomies. Considering only spectral features, the initial accuracy was about 71.3%. The spectral texture improved the classification accuracy to 73.8%. Spectral texture was responsible for reducing the misclassification between grassland physiognomies (Open Grassland and Shrubby Grassland). However, the texture based on GLCM entropy extracted from NDVI and SLMM components, especially vegetation, improved even more the classification

accuracy reaching 74.3%. They not only reduced the confusion between grassland physiognomies mentioned before but also increased the discrimination of Shrubby Grassland and Shrubby Savanna. Gallery Forests had high accuracy on all cases. As future works, we suggest using temporal data analysis and combining spectral texture with NDVI and SLMM textures.

5 References

- Blackbridge – **Satellite Imagery Product Specifications**, 2015. Available at: www.e-geos.it/images/Satellite_data/RAPIDEYE/RE_Product_Specifications_ENG.pdf. Accessed aug 04. 2016.
- Breiman, L. Random forests. **Machine Learning Journal**, v.45, p.5-32, 2001.
- Carvalho, L.; Rahman, M.; Hay, G.; Yackel, J. Optical and SAR imagery for mapping vegetation gradients in Brazilian savannas: Synergy between pixel-based and object-based approaches. In: International Conference of Geographic Object-Based Image, 38, 2010, Ghent, Belgium. **Proceedings...** 2010, p.1-7.
- Chen, K.; Jacobson, C.; Blong, R. Using NDVI image texture analysis for bushfire-prone landscape assessment. In: Asian Conference on Remote Sensing, 22, 2001, Venue, Singapore. **Proceedings...** 2010. p.9.
- Costa, W.S.; Fonseca, L.M.G.; Kosting, T.S. Mapping Grasslands Formations and Cultivated Pastures in the Brazilian Cerrado Using Data Mining. In: GeoProcessing - International Conference on Advanced Geographic Information Systems and Applications, 6, 2014, Barcelona, Spain, **Proceedings...** 2014. p.138-141.
- Ferreira, L.G.; Yoshioka, H.; Hueta, A.; Sano, E. E. Seasonal landscape and spectral vegetation index dynamics in the Brazilian Cerrado: An analysis within the Large-Scale Biosphere–Atmosphere Experiment in Amazônia (LBA). **Remote Sensing of Environment**, v.87, n.4, p.534-550, 2003.
- Ferreira, M.E.; Ferreira, L.G.; Sano, E. E.; Shimabukuro, Y.E. Spectral linear mixture modeling approaches for land cover mapping of tropical savanna areas in Brazil. **International Journal of Remote Sensing**, v.2, n.28, p.413-429, 2007.
- Hall, M.A.; Frank, E.; Holmes, G.; Pfahringer, B.; Reutemann, P.; Witten, I.H. The WEKA Data Mining Software: An Update. **SIGKDD Explorations**. New York, v.11, n.1, p.10-18, 2009.
- Haralick, R.M.; Shanmugam, K.; Dinstein, I. textural features for image classification. **IEEE Transactions on systems, man, and cybernetics**, n.6, p.610-621, 1973.
- Klink, C.; Machado, R. Conservation of the Brazilian Cerrado. **Conservation Biology**, v.19, n.3, p.707-713, 2005.
- Liesenber, V.; Ponzoni, F.J.; Galvão, L.S. Análise da dinâmica sazonal e separabilidade espectral de algumas fitofisionomias do Cerrado com índices de vegetação dos sensores Modis Terra e Aqua. **Revista Árvore**, v.31, n.2, p.295-305, 2007.
- Ministério do Meio Ambiente (MMA) – **PPCerrado – Plano de ação para prevenção e controle do desmatamemtno e das queimadas no cerrado: 2ª fase (2014-2015)**,

2014. Available at: http://www.florestal.gov.br/snif/imagens/Publicacoes/ppcerrado_2fase.pdf. Accessed aug. 04. 2016.
- Ministério do Meio Ambiente (MMA) – **Mapeamento do uso e cobertura do Cerrado: Projeto TerraClass Cerrado 2013**, 2015. Available at: <http://www.mma.gov.br/publicacoes/biomas/category/62-cerrado>. Accessed aug. 05. 2016.
- Ning, H.A.N.; Jing, W.U.; Tahmassebi, A.R.S.; XU, H.W.; Ke, W.A.N.G. NDVI-based lacunarity texture for improving identification of torreyia using object-oriented method. **Agricultural Sciences in China**, v.10, n.9, p.1431-1444, 2011.
- Nussbaum, S.; Menz, G. **Object-based image analysis and treaty verification: new approaches in remote sensing-applied to nuclear facilities in Iran**. Springer Science & Business Media, 2008. 172 p.
- Oliveira, L.T.; Oliveira, T.C.A.; Carvalho, L.M.T.; Lacerda, W.S.; Campos, S.R.S.; Martinhago, A.Z.. Comparison of machine learning algorithms for mapping Phytophysionomies of the Brazilian Cerrado. In: Brazilian Symposium on GeoInformatics, 9, 2007, Campos do Jordão, SP. **Anais...**, 2007. p.195-205.
- Peneque-Galvez, J.; Mas, J.F.; Moré, G.; Cristobál, J.; Orta-Martinez, M.; Luz, A.C.; Guéze, M.; Macía, M.J.; Reyes-Garcia, V. Enhanced land use/cover classification of heterogeneous tropical landscapes using support vector machines and textural homogeneity. **International Journal of Applied Earth Observation and Geoinformation**, v.23, n.1, p.372-383, 2013.
- Ribeiro, J.F.; Walter, B.M.T. As principais fitofisionomias do Bioma Cerrado. In: Sano, S.M.; Almeida, S.P.; Ribeiro, J.F. **Cerrado: ecologia e flora**. Brasília: EMBRAPA, 2008. p.152-212.
- Sano, E.E.; Rosa, R.; Brito, J.L.S.; Ferreira, L.G.; Bezerra, H.S. Mapeamento da cobertura vegetal natural e antrópica do bioma Cerrado por meio de imagens Landsat ETM+ In: Simpósio Brasileiro de Sensoriamento Remoto, 14, 2009, Natal, RN. **Anais...**, 2009. p.1199-1206.
- Schwieder, M.; Leitão, P.J.; Bustamante, M.M.C.; Ferreira, L.G.; Rabe, A.; Hostert, P. Mapping Brazilian savanna vegetation gradients with Landsat time series. **International Journal of Applied Earth Observation and Geoinformation**, v.52, p.361-370, 2016.
- Shimabukuro, Y.E.; Smith, J.A. The least-squares mixing models to generate fraction images derived from remote sensing multispectral data, **IEEE Transactions on Geoscience and Remote Sensing**, v.29, n.1, p.16-20, 1991.
- Tucker, C.J. Red and photographic infrared linear combinations for monitoring vegetation. **Remote Sensing of Environment**, v.8, n.2, p.127-150, 1979.